FULL PAPER

Dalton
www.rsc.org/dalton

New self-assembled one-dimensional nickel coordination polymers and hydrogen-bonded networks

Dejana Vujovic,[a] Helgard G. Raubenheimer[a] and Luigi R. Nassimbeni[b]

[a] *Department of Chemistry, University of Stellenbosch, Private Bag X1, Matieland 7602, South Africa*

[b] *Department of Chemistry, University of Cape Town, Rondebosch 7701, South Africa*

Received 9th July 2002, Accepted 4th December 2002
First published as an Advance Article on the web 23rd January 2003

Reaction of $Ni(NCS)_2$ with aminobenzonitrile (ABN) isomers in solution gave rise to the formation of five coordination polymers of the general formula $[Ni(NCS)_2(ABN)_2]_n$ consisting of one-dimensional chains with adjacent nickel centres linked by bridging NCS^- or ABN ligands. The compounds were characterised by single crystal X-ray diffraction, X-ray powder diffraction, infrared spectroscopy, thermogravimetry, differential scanning calorimetry and mass spectrometry.

Introduction

Formation of self-assembled coordination polymers, zeolitic structures and hydrogen-bonded networks has attracted considerable interest in recent years. The main attractions of extended structures lie in their tunability and many potential applications. The diversity of possible architectures is due to the various parameters known to affect the final geometry of the supramolecular systems. The architectures are tuned and influenced by utilising different coordination environments of the metal centres, a large number of rigid and flexible organic ligands to choose from, position and type of functional groups on the ligands, choice of counter ions, solvents, as well as the solution pH-value and crystallisation conditions. This can affect the size, shape and hydrophilic character of voids in the zeolitic structures and hydrogen-bonded networks as well as the overall stability of the supramolecular systems. Some of the well-known geometries of the coordination polymers are ladder, square grid, diamondoid, T-shape, honeycomb and brick. Apart from the scientific interest, the targeted compounds are engineered with specific applications in mind such as: separation and selective inclusion, ion exchange, catalysis, magnetism, non-linear optical properties and sensing. Some of the recent papers covering the points mentioned above are given in references 1–16.

For this study we chose two types of ligands namely thiocyanate and aminobenzonitrile isomers for coordination with Ni(II) as they allow formation of the number of structurally different compounds. Thiocyanate can coordinate to a metal centre as a monodentate ligand through its sulfur or nitrogen atom, as an end-to-end bridging ligand between two metal centres utilising both S and N atoms or as a single atom bridging ligand. Aminobenzonitrile isomers have similar capabilities for bonding where either amine or cyanate nitrogen can bond to a metal atom. This allows them to act as monodentate ligands coordinated through one of the two nitrogen groups, bidentate ligands in the case of 2-aminobenzonitrile and bridging ligands between two metal centres when both nitrogen atoms are coordinated. The amine group in conjunction with cyanate and thiocyanate moieties also allows for the formation of hydrogen-bonded networks. We investigated how Ni(II) would respond when presented with all these possibilities and, in addition, with isomers of aminobenzonitrile.

Here we report the formation of self-assembled coordination polymers and hydrogen-bonded networks using $Ni(NCS)_2$ solutions and the three ligands namely 4-, 3- and 2-aminobenzonitrile (4ABN, 3ABN and 2ABN) respectively. A CSD search yielded only four complex compounds with aminobenzonitriles and, to our knowledge, we report here the first coordination polymers with ABN ligands. Three polymeric structures $[Ni(NCS)_2(4ABN)_2]_n$ (**1**), $[Ni(NCS)_2(3ABN)_2]_n$ (**2**) and $[Ni(NCS)_2(2ABN)_2]_n$ (**3**) and two host–guest systems $\{[Ni(NCS)_2(4ABN)_2]\cdot(4ABN)\}_n$ (**4**) and $\{[Ni(NCS)_2(3ABN)_2]\cdot C_6H_6\}_n$ (**5**) were identified.

Experimental

Preparation of $[Ni(NCS)_2(4ABN)_2]_n$ (1), $[Ni(NCS)_2(3ABN)_2]_n$ (2) and $[Ni(NCS)_2(2ABN)_2]_n$ (3)

The chosen aminobenzonitrile isomer (0.354 g, 3 mmol) was dissolved in 3 ml ethanol. The resultant solution was added to 5 ml of a 0.2 mmol ml^{-1} ethanolic $Ni(NCS)_2$ solution. The mixtures were left to evaporate slowly and dark green crystals of $[Ni(NCS)_2(4ABN)_2]_n$ and $[Ni(NCS)_2(3ABN)_2]_n$ formed within 48 h. Crystals of $[Ni(NCS)_2(2ABN)_2]_n$ suitable for X-ray diffraction study were very difficult to grow. Therefore, the final solution was filtered using 0.45 μm nylon filters, the vials covered with parafilm and light blue crystals obtained after three to four weeks in very small quantities. Changing the crystal growth conditions in any way resulted in a powdery $[Ni(NCS)_2(2ABN)_2]_n$ product and no crystalline inclusion compounds could be isolated. Elemental analysis: Calc. for $NiC_{16}H_{12}N_6S_2$: C 46.74, H 2.94, N 20.44, S 15.60. Found: for **1**: C 46.89, H 3.01, N 20.27, S 15.43. For **2**: C 47.0, H 2.83, N 20.52, S 15.41. For **3**: C 46.71, H 2.80, N 20.37, S 15.64%.

Preparation of the inclusion compound $\{[Ni(NCS)_2(4ABN)_2]\cdot(4ABN)\}_n$ (4)

The clathrate was prepared as described above except that the $Ni(NCS)_2$ to 4ABN ratio was increased from 1 : 3 to 1 : 10. Dark blue crystals formed after 4–6 weeks. Elemental analysis: Calc. for $NiC_{23}H_{18}N_8S_2$: C 52.19, H 3.43, N 21.17, S 12.12. Found: C 51.73, H 2.96, N 21.51, S 12.62%.

Preparation of the inclusion compound $\{[Ni(NCS)_2(3ABN)_2]\cdot C_6H_6\}_n$ (5)

3ABN (0.591 g, 5 mmol) and 0.391 g (5 mmol) of benzene were dissolved in 3 ml of ethanol and added to 5 ml of a 0.2 mmol ml^{-1} ethanolic solution of $Ni(NCS)_2$. The resultant crystalline sample consisted of a mixture of differently coloured crystals. The majority were light blue in colour representing compound **2** while a small amount of dark blue crystals of **5** also formed. Suitable quality crystals were grown by slow evaporation over a period of 24 h for **2** and after 48 h for **5**. Elemental analysis: Calc. for $NiC_{22}H_{18}N_6S_2$: C 54.01, H 3.71, N 17.18, S 13.11. Found: C 53.88, H 3.50, N 16.98, S 12.76%.

DOI: 10.1039/b206638f

Table 1 Crystallographic data for compounds **1**–**5**

Compound	**1**	**2**	**3**	**4**	**5**
Empirical formula	$NiC_{16}H_{12}N_6S_2$	$NiC_{16}H_{12}N_6S_2$	$NiC_{16}H_{12}N_6S_2$	$NiC_{23}H_{18}N_8S_2$	$NiC_{22}H_{18}N_6S_2$
Formula weight	411.15	411.15	411.15	529.28	489.26
T/K	173(2)	173(2)	173(2)	173(2)	173(2)
Crystal system	Monoclinic	Monoclinic	Monoclinic	Monoclinic	Monoclinic
Space group	$P2_1/c$	$C2/c$	$C2/c$	$P2_1/n$	$P2_1/c$
a/Å	5.5903(2)	16.9554(3)	22.1014(7)	9.3711(1)	8.6743(5)
b/Å	24.6665(1)	5.5542(1)	7.5459(3)	13.2207(1)	7.2741(5)
c/Å	12.7539(5)	18.2897(3)	11.1386(5)	19.522(1)	17.4386(12)
β/°	100.465(2)	92.491(1)	113.440(2)	95.903(1)	99.754(2)
V/Å^3	1729.4(1)	1720.8(1)	1704.3(1)	2403.2(1)	1084.4(1)
Z	4	4	4	4	2
D_c/Mg m^{-3}	1.579	1.587	1.602	1.463	1.498
μ/mm^{-1}	1.375	1.381	1.395	1.010	1.109
F(000)	840	840	840	1088	1008
Reflections collected	6633	5462	3494	5476	4183
Unique reflections	3885 [R_{int} = 0.037]	2120 [R_{int} = 0.018]	1958 [R_{int} = 0.031]	4387 [R_{int} = 0.034]	2352 [R_{int} = 0.034]
Data/restraints/parameters	3885/0/242	2120/0/123	1958/0/123	4387/0/331	2352/0/144
R ($I > 2\sigma(I)$)	0.0477	0.0226	0.0326	0.0305	0.0407
R (all data)	0.0917	0.0254	0.0526	0.0467	0.0767
wR' ($I > 2\sigma(I)$)	0.0975	0.0587	0.0652	0.0649	0.0876
wR' (all data)	0.1066	0.0602	0.0708	0.0704	0.0987

Thermal analysis

Thermogravimetry (TG) and differential scanning calorimetry (DSC) were carried out on a Perkin Elmer PC7-Series system. The experiments were performed over a temperature range of 30–300 °C at a heating rate of 20 °C min^{-1} with a purge of dry nitrogen flowing at 30 ml min^{-1}. The samples were crushed, blotted dry and placed in open platinum pans for TG experiments and in crimped but vented aluminium pans for DSC.

Structure determination

Cell dimensions were obtained from the intensity data measurements on a Nonius Kappa CCD diffractometer using graphite-monochromated Mo-Kα radiation (λ = 0.71069 Å). The strategy for the data collection was evaluated using the COLLECT[17] software. For all five structures data were collected at 173(2) K and by the standard ϕ-scan and ω-scan techniques. In each case all sets of data were scaled and reduced using DENZO-SMN.[18] The structures were solved by direct methods using SHELX-86[19] and refined employing full-matrix least-squares with the program SHELX-97[20] refining on F^2. Program X-Seed[21] was used as a graphical interface for structure solution and refinement using SHELX. No absorption corrections were necessary. The important crystal and experimental data for all five structures are given in Table 1.

CCDC reference numbers 189528–189532.

See http://www.rsc.org/suppdata/dt/b2/b206638f/ for crystallographic data in CIF or other electronic format.

Elemental analysis

Elemental analysis was carried out to determine the percentage of C, H, N and S using a Carlo Erba 1106 Elemental Analyser. For each sample the analysis was carried out in duplicate. In the case of inclusion compounds the samples were kept in mother liquor until analysis was performed and then blotted dry on filter paper. The inclusion compounds were not dried under vacuum prior to analysis so as to avoid the possibility of guest loss.

Infrared spectroscopy

The IR spectra were recorded using a Perkin Elmer 983 IR spectrophotometer and NaCl plates. Samples were run as Nujol mulls over the range 4000–400 cm^{-1} and analysed for the mode of thiocyanate coordination.

X-Ray powder diffraction (XRPD)

X-ray powder diffraction patterns were measured using a Philips PW1050/25 goniometer with nickel-filtered Cu-Kα radiation. Samples were packed in aluminium sample holders and a step size of 0.1° at a scan rate of 1 s per step in the 2θ range from 6 to 40° was employed for analysis. Calculated XRPD traces were generated from the crystal structure solutions using program LAZYPULVERIX[22] for comparison purposes.

Matrix-assisted laser desorption ionisation-time of flight (MALDI-TOF) mass spectrometry

The analysis of polymer samples in solution was performed using a Perseptive Biosystems DE-PRO MALDI mass spectrometer employing an N_2 laser and 1,8-dihydroxy-9[10*H*]-anthracenone matrix using ethanol as a solvent. Each sample was analysed as soon as it was prepared and also 24 h later before crystalline material appeared. Mass spectra were recorded for compounds **1**, **2** and **3**, which were prepared as described earlier.

Results and discussion

Crystal structure analysis

Crystal structure analysis of compounds **1**–**5** revealed that one-dimensional double stranded chain polymers were formed. In each polymer the metal to ABN ratio is 1 : 2 giving rise to the same general formula $[Ni(NCS)_2(ABN)_2]_n$. The five polymers were found to differ in at least one of the following: the bridging ligand, orientation of ligands around the metal centres or orientation of adjacent octahedral units. In all the products the nickel atoms contained *trans*-coordinated amine groups of an ABN and two N-bonded thiocyanate ligands appearing *cis* (in **1** and **2**) or *trans* (in **3**–**5**) to each other (Scheme 1, **I** and **II** respectively). Conceptually, self-association of such four coordinate complexes occurs by anti-symbiotic coordination of their two thiocyanate S atoms (**1** and **2**) or by coordination of dangling ABN nitrile groups. The latter interaction mode is applicable to complexes **3**–**5** involving one ABN ligand from each of two neighbouring nickel complexes. Although the amine group of ABN is preferred in **1** and **2** where bridging involves NCS^- ligands, the Ni–NC bond distances of bridging ABN in complexes **3**–**5** are consistently shorter than the Ni–NH_2 separations.

Table 2 Hydrogen-bonding parameters

Compound	Donor (D)	Acceptor (A)	D–H/Å	D···A/Å	D–H···A/°
1	N(7A)	S(1D)[1]	0.90(4)	3.628(4)	178(3)
	N(7B)	N(9B)[2]	0.90(4)	3.079(5)	164(4)
2	N(7A)	N(9A)[3]	0.82(1)	3.125(2)	171(2)
3	—	—	—	—	—
4	N(7A)	S(3D)[4]	0.88(2)	3.417(2)	152(2)
	N(7A)	N(9G)[5]	0.85(2)	3.012(2)	175(2)
	N(7B)	S(3C)[6]	0.87(2)	3.408(2)	167(2)
	N(7G)	S(3C)[7]	0.83(3)	3.541(2)	169(2)
	N(7G)	S(3D)[8]	0.85(3)	3.516(2)	166(2)
5	N(7A)	S(1)[9]	0.94(1)	3.454(2)	145(2)

[1] $-x+1, -y, -z$. [2] $x-1, -y-1/2, z-1/2$. [3] $-x, y+1, -z+3/2$. [4] $-x+3/2, y-1/2, -z+1/2$. [5] $x-1, y, z$. [6] $-x+1, -y+1, -z$. [7] $-x+3/2, y+1/2, -z+1/2$. [8] $-x+2, -y+1, -z+1$. [9] $x, y-1, z$.

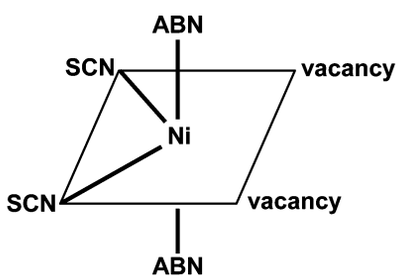

I

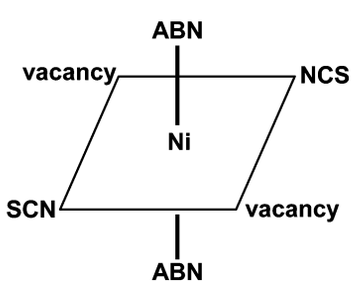

II

Scheme 1

Details of hydrogen bonding in all compounds are summarised in Table 2.

Nickel ion coordination for **1** is shown in Fig. 1. The Ni-$(NCS)_2(4ABN)_2$ monomer units are located in general positions. The polymer chain is propagated through two thiocyanate groups connecting adjacent metal centres through their nitrogen and sulfur atoms. The coordination polymer runs parallel to the crystallographic *a*-axis. The metal–metal distance between adjacent nickel centres within one polymer strand is equal to the length of the *a*-axis (5.59 Å) while the closest Ni–Ni distance between two neighbouring strands is 6.30 Å. The non-bridging 4ABN ligands are bonded through their amine groups to the nickel atoms. On each monomer unit they face the same way with the torsion angle [C(8A)–N(7A)–N(7B)–C(8B)] being 19.7°. The ligands (and the aromatic rings) on the axial positions of the upper as well as the lower polymer rims are parallel to each other. This was also observed for compounds **2**, **4** and **5**. However for compound **3**, the repeating NCS^- ligands are gauche, so that if we consider adjacent nickel ions, Ni(1) and Ni(1)′ which translate half a unit cell length along *c*, we may define a torsion angle [S(1)–Ni(1)–Ni(1)′–S(1)′] which has a value of 59.6°. The polymer strands of **1** are interconnected in three dimensions by an extensive network of N–H ··· N and N–H ··· S hydrogen bonds with an amine group of one polymer strand acting as a proton source and the N and S partners are from the nitrile and thiocyanate moieties of another strand (Fig. 2).

The arrangement of ligands around the metal centres in the coordination polymer **2** is shown in Fig. 3. The monomer units are located on the centres of inversion at Wyckoff position *a*.

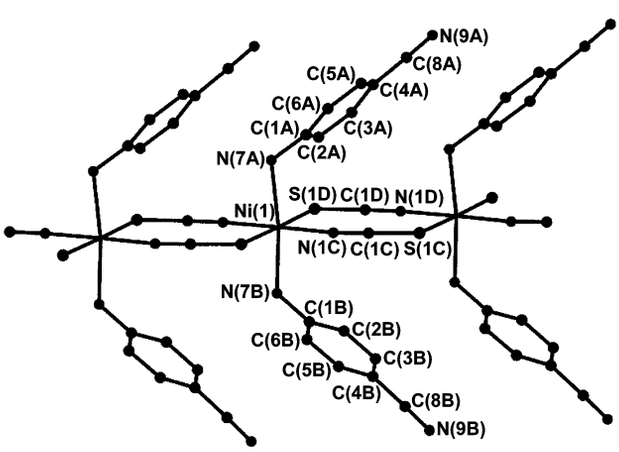

Fig. 1 Polymer **1**, showing the numbering scheme.

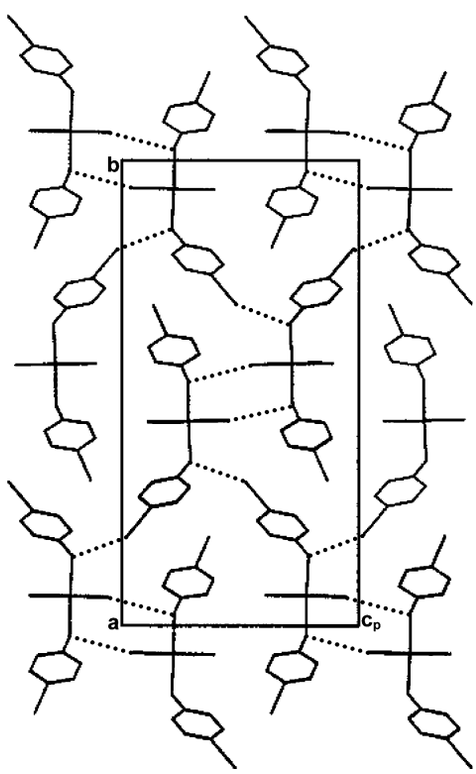

Fig. 2 Packing diagram for **1** down [010] with hydrogen bonding shown as dotted lines.

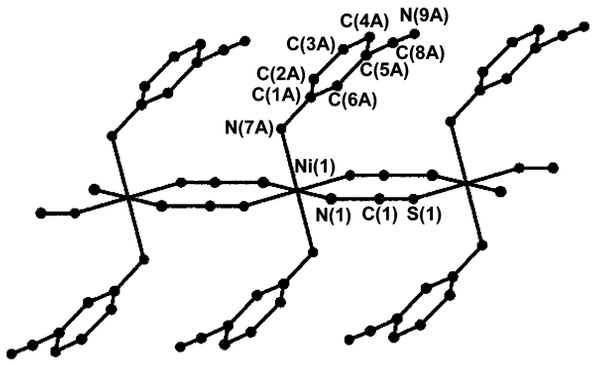

Fig. 3 Polymer **2**, showing the numbering scheme.

The polymer strands run parallel to the crystallographic *b*-axis. As in the case of **1**, the polymer chain is propagated through two NCS^- groups with the separation of adjacent nickel centres 5.55 Å (the length of the *b*-axis). The closest metal–metal distance between two polymer strands is 8.91 Å. N–H ··· N hydrogen bonding was observed between the adjacent polymer units giving rise to infinite hydrogen-bonded sheets parallel to the (011) plane.

Polymer **3** differs from **1** and **2** and its structure is depicted in Fig. 4. The nickel ions are again located on the centres of inversion at Wyckoff position *a*. Here the adjacent nickel centres are connected through two 2ABN molecules and the NCS^- ligands occupy two *trans* positions perpendicular thereto. The polymer chains are parallel to the crystallographic *c*-axis with the distance between adjacent nickel atoms being 5.57 Å and the shortest nickel–nickel distance between two polymer strands is 7.55 Å. Interactions of the π ··· π type are present between the aromatic rings of the ABN ligands with the shortest perpendicular distance of 3.513 Å and a dihedral angle of 32.71°. No conventional hydrogen bonds are seen in this compound.

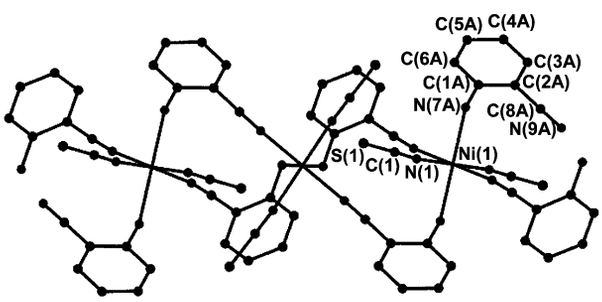

Fig. 4 Polymer **3**, showing the numbering scheme.

In the inclusion compound **4** a dramatic change occurs compared to **1** that contains the same ABN ligands. Now the coordination polymer is formed by two 4ABN ligands bridging the pairs of Ni atoms while NCS^- groups are coordinated at the axial positions like in **3** (Fig. 5). Both the host and the guest species occupy general positions with the polymer chains parallel to the *a*-axis. The host polymer units pack to form channels running in the [100] direction in which the 4ABN guest molecules are located (Fig. 6). The cross-sectional area of the channels was measured using program SECTION[23] and it varies between 10.9 × 8.6 Å² and 7.8 × 3.1 Å². The polymer strands are hydrogen-bonded to each other (N–H ··· S) giving rise to hydrogen-bonded tubular structures. Again π ··· π interactions are present now between 4ABN molecules in the polymer strands and also between the guest molecules with distances between the centres of gravity of the aromatic rings 3.430 Å and 3.460 Å, respectively. The positions of guest molecules are stabilised in the channels by means of N–H ··· S and N–H ··· N host–guest hydrogen bonding.

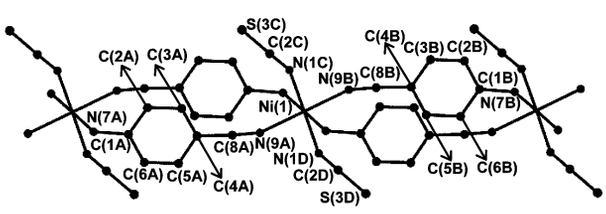

Fig. 5 Polymer in inclusion compound **4**, showing the numbering scheme.

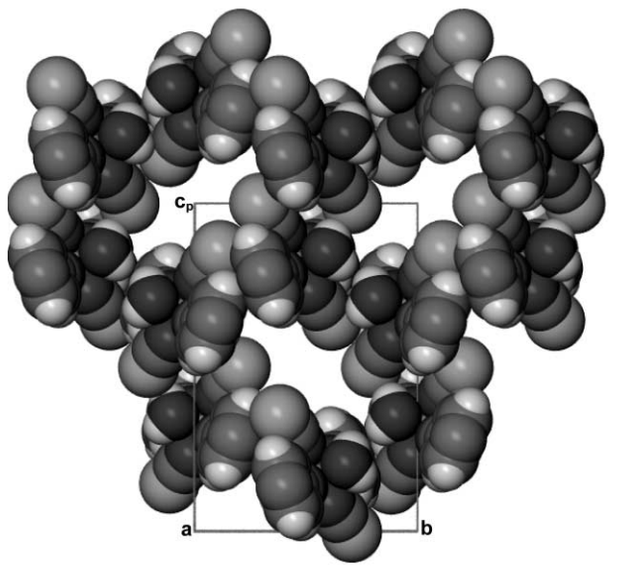

Fig. 6 Space-filling projection of **4** along [100] with guest molecules omitted, showing the open channels.

Inclusion of 3ABN in compound **5**, with the same constitution as **2**, again changes the coordination modes and the polymeric chains are created by connecting adjacent Ni(II) ions by means of two 3ABN ligands with axial positions occupied by thiocyanates. The coordination polymers run parallel to the *a*-axis. Both host and guest species are located on the centres of inversion at Wyckoff positions *a* and *d*, respectively. The packing diagram in Fig. 7 shows that the polymer strands form

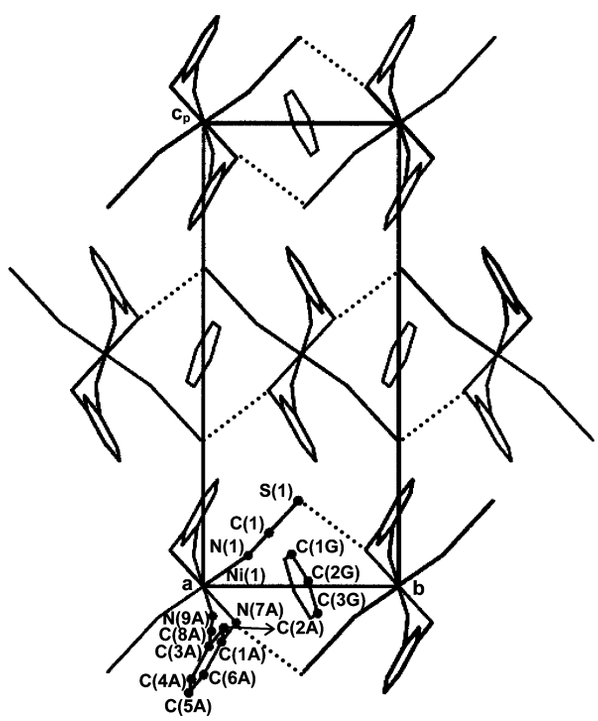

Fig. 7 Packing diagram for **5** down [100] with hydrogen bonding (dotted lines) and the numbering scheme.

Table 3 Selected bond lengths and angles for compounds **1**–**5**

	Bond length/Å		Bond angle/°	
1	Ni–NCS	1.999(3)–2.020(3)	N–C–S	178.7(1)–179.4(4)
	Ni–SCN	2.489(1)–2.528(1)	Ni–N(H_2)–C	120.5(2)–122.0(2)
	Ni–NH_2	2.144(3)–2.151(3)	N–Ni–N	85.7(1)–93.8(1)
			N–Ni–S	86.3(1)–94.0(1)
2	Ni–NCS	2.016(1)	N–C–S	179.3(1)
	Ni–SCN	2.544(1)	Ni–N(H_2)–C	118.8(1)
	Ni–NH_2	2.137(1)	N–Ni–N	86.0(1)–94.1(1)
			N–Ni–S	87.0(1)–93.0(1)
3	Ni–NCS	2.030(2)	N–C–S	179.1(2)
	Ni–NC	2.101(2)	Ni–N(H_2)–C	121.3(1)
	Ni–NH_2	2.163(2)	N–Ni–N	86.3(1)–93.7(1)
4	Ni–NCS	2.025(1)–2.033(1)	N–C–S	177.7(2)–179.9(2)
	Ni–NC	2.077(1)–2.085(1)	Ni–N(H_2)–C	115.9(1)–117.3(1)
	Ni–NH_2	2.177(1)–2.181(1)	N–Ni–N	85.9(1)–93.6(1)
5	Ni–NCS	2.044(2)	N–C–S	179.4(3)
	Ni–NC	2.096(2)	Ni–N(H_2)–C	120.7(2)
	Ni–NH_2	2.155(2)	N–Ni–N	86.0(1)–94.0(1)

hydrogen-bonded (N–H ··· S) sheets parallel to the (110) plane. The sheets contain channels down the *a*-axis in which benzene guests are located. The channels are hour-glass in shape and could almost be described as pockets. The channel size varies between 7.2 × 4.0 Å^2 at the widest parts and 2.6 × 1.5 Å^2 at the narrowest parts.

XRPD patterns were measured for all compounds to determine whether the crystals chosen for the single crystal X-ray analyses were representative of the whole sample. For the product mixture of **5**, consisting of light blue (compound **2**) and dark blue (compound **5**) crystals, the two sets of crystals were mechanically separated before XRPD traces were recorded. In all five cases the calculated and experimental XRPD traces were in agreement with all the peaks present at the correct angular positions and with correct relative intensities. Elemental analysis was also performed on all compounds and the experimental C, H, N and S percentages are in agreement with the calculated values.

In agreement with the single crystal X-ray analyses we were able to identify the modes of thiocyanate coordination in all five compounds using IR spectroscopy. In the case of **1** and **2**, where NCS^- ligands act as end to end bridging groups, the CN stretching vibrations[24] should be greater than 2100 cm^{-1}. This proved to be the case with ν(CN) values of 2107 and 2119 cm^{-1} for **1** and **2**, respectively. Nitrogen-bonded NCS^- complexes have a CN stretching frequency[24] near or below 2070 cm^{-1}. In **3**, **4** and **5** with the thiocyanates bonded only through the nitrogen atoms to the nickel, the ν(CN) stretching frequencies were found at 2075, 2076 and 2071 cm^{-1}, respectively.

Compounds **1**–**5** show many interesting and some rarely observed characteristics. The double NCS^- bridges connecting adjacent nickel atoms in **1** and **2** are unusual and out of 1013 structures in the CSD containing the M(NCS)$_2$ fragment (where M is any metal), only five have this feature. Metal compounds with bridging NCX groups (X = O, S, Se) are of interest due to their possible magnetic properties and recently the nickel(II) coordination polymer, Ni(NCS)$_2$(imidazole)$_2$, that contains double thiocyanate bridges was shown to exhibit long-range magnetic ordering.[25] Compounds **3**, **4** and **5** represent the first examples of coordination polymers with donor groups connected *via* rigid aromatic units and acting as double bridges. Table 3 contains selected bond lengths and angles involving the nickel centre and all the values are typical for these types of interactions. The values also indicate that the monomer units have irregular octahedral geometry.

Thermal analysis

The thermal analysis results are summarised in Table 4 and representative traces are presented in Fig. 8. For compounds **1**, **2** and **3**, the TG and DSC traces have the same profiles (Fig. 8(a)). In each case the TG trace consists of a one-step mass loss due to the loss of two ABN ligands and a corresponding endotherm in the DSC trace. The inclusion compounds **4** and **5** exhibit two mass loss steps in the TG with two matching endotherms (A and B) in the DSC (Fig. 8(b)). The first mass loss and endotherm A are due to the guest release with the second mass loss and endotherm B being due to the loss of two ABN ligands.

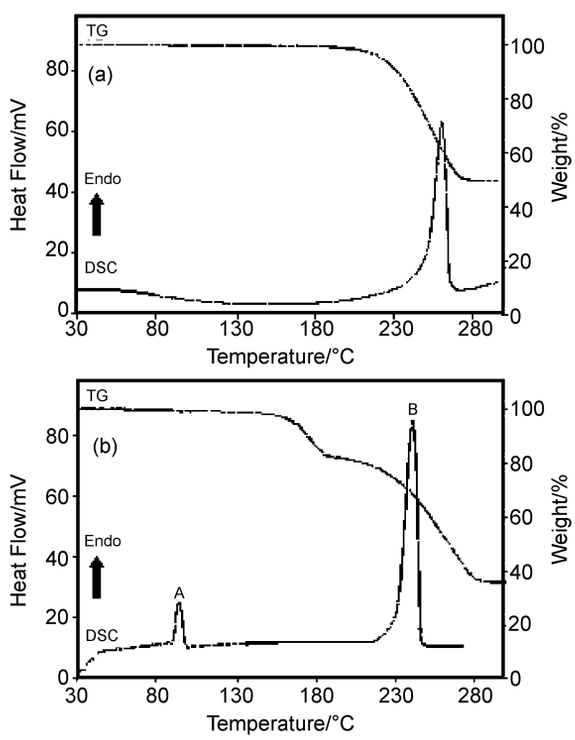

Fig. 8 TG and DSC results for **2** (a) and **5** (b).

The onset temperature (T_{on}) of the thermal reaction and the corresponding ΔH value can be used alone or in conjunction with the melting and boiling points and channel sizes to determine the relative stability of the compounds studied. For example, in the study of the separation of aminobenzonitrile

Table 4 Thermal analysis data

Compound			1	2	3	4	5
M : L : G ratio			1 : 2 : 0	1 : 2 : 0	1 : 2 : 0	1 : 2 : 1	1 : 2 : 1
TG Results	Total mass loss (%) (found)		57.9	57.3	57.7	66.4	64.0
	Total mass loss (%) (calc.)		57.5	57.5	57.5	66.9	64.3
DSC Results	Peak 1 (guest loss)	T_{on}/K	—	—	—	406.4	363.1
	Peak 2	T_{on}/K	530.2	522.2	453.1	503.7	500.3
	ΔH/kJ mol^{-1}	Peak 1/peak 2	–/87.0	–/83.3	–/74.3	3.1/70.0	1.2/74.2
Ligand melting point/K			358.5	325.5	320.5	358.5	325.5
Guest melting point (T_{mp})/K			—	—	—	358.5	278.5
$T_{on} - T_{mp}$ for guest loss			—	—	—	47.9	87.6

isomers using 1,1,6,6-tetraphenylhexa-2,4-diyne-1,6-diol we demonstrated that T_{on}, ΔH and lattice energy values correlated well with the solid–solid reactions, displacement reactions and competition experiments results.[26] The comparison of the T_{on} and ΔH values corresponding to the loss of ABN ligands in compounds **1**–**5** can be employed to give an indication of the relative stability of the polymeric chains. These values suggest that **1** and **2** are more stable polymers than compounds **3**–**5**. This is further verified by comparing the thermal parameters for **1** *vs.* **4** and **2** *vs.* **5**. In each set the polymers consist of the same ligands differently coordinated around the nickel centre (bridging NCS^- *vs.* bridging ABN groups). Changing from bridging NCS^- groups to ABN ligands, a decrease in the T_{on} and ΔH values indicates decreased thermal stability. This trend is observed despite the fact that aminobenzonitriles act as monofunctional ligands in **1** and **2** and as bridging ligands in **3**–**5** and, therefore, the loss of one ABN ligand in **1** and **2** requires breaking of one Ni–NH_2 bond which should be energetically less demanding than the loss of one ABN ligand in compounds **3**–**5** which require two bonds to be ruptured (Ni–NH_2 and Ni–NC).

It has also previously been shown that the parameter $T_{on} - T_{bp/mp}$ (where bp and mp are boiling and melting points, respectively, of the guest) gives an indication of stability in the host–guest systems.[27] When the T_{on} value is higher then the boiling point of a given liquid guest or higher than the melting point of a solid guest, the guest is held more tightly in the crystal rendering the inclusion compound more stable. This suggests that benzene guest molecules in compound **5** are held more tightly in the channels than the 4ABN guest molecules in **4**. This result is in agreement with the channel size analysis. We have shown that the channels in **5** are more constricted than the channels in **4** and, therefore, they produce a greater barrier to guest desorption rendering the host–guest system more stable. This kind of analysis is of importance in the study of reagent storage and recently calix[4]arene was successfully employed for storage of methane and freon compounds.[28] The resultant inclusion compounds were found to be remarkably stable with $T_{on} - T_{bp}$ values of 260 °C for CF_3Br, 370 °C for CF_4 and 320 °C for CH_4. The boiling points of CF_3Br, CF_4 and CH_4 are −57.7, −127.9 and −160 °C, respectively.

MALDI-TOF MS

MALDI-TOF MS is a mild technique employed in the characterisation of compounds ranging from low molecular mass polymers to polysaccharides, nucleic acids and proteins as large as 300 kDa. The instrument is very sensitive and allows the detection of subpicomolar amounts of analytes with a precision of 20 ppm. Some of the problems encountered in the study of coordination polymers are that they are often difficult to crystallise, have low solubility, low molecular mass and are often found to decompose in solution.[29–32] The study is, therefore, important in order to determine if the structure and degree of polymerisation are the same in solution and solid state.

The analysis of solutions of **1**, **2** and **3** produced identical results and a representative mass spectrum is shown in Fig. 9.

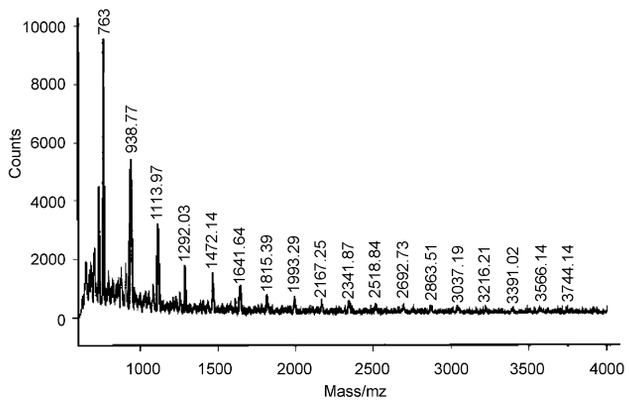

Fig. 9 Mass spectrum for solution of **1**.

The molecular mass difference between consecutive peaks is approximately 175 which corresponds to the molecular mass of $Ni(NCS)_2$ (M_r = 174.8). The results indicate that solutions **1**, **2** and **3** contain $[Ni(NCS)_2]_n$ polymers with $1 \leqslant n \leqslant 21$. The results were reproducible over time and with different sample batches suggesting that strong and variable coordination of ABN ligands onto the nickel centres and thus the formation of $[Ni(NCS)_2(ABN)_2]_n$ polymers is a solid state process and that these compounds are probably not polymeric in solution.

Conclusion

Five new one-dimensional chain polymers were prepared by self-assembly. The coordination of ligands around the metal centres proved to be sensitive to the position of functional groups on the ABN ligands and introduction of the guest species to the structures. The relatively small discriminating nature of the two ligand types (ABN and NCS^-) employed in bridging capacity as well as the concomitant change of the two thiocyanates being *cis* or *trans*, are clearly illustrated by the fact that such changes result by inclusion of ABN or benzene in the crystals formed.

Thermal stability of the polymers was determined by thermal analysis and the onset temperatures of thermal degradation vary between 180.1 and 257.5 °C. The polymer structures where NCS^- moieties act as bridges between nickel ions (**1** and **2**) were shown to be more stable than the compounds where aminobenzonitriles act as bridging groups. We are currently studying systems with the same ligands but different M(II) metal centres in order to gain a greater insight into reasons behind the variable geometry of these coordination polymers.

Acknowledgements

We would like to thank the Claude Harris Leon foundation for financial support.

References

1 B. Moulton and M. J. Zaworotko, *Chem. Rev.*, 2001, **101**, 1629.
2 G. F. Swiegers and T. J. Malefetse, *Chem. Rev.*, 2000, **100**, 3483.

3 M. J. Zaworotko, *J. Chem. Soc., Chem. Commun.*, 2001, 1.
4 T. Kuroda-Sowa, T. Horino, M. Yamamoto, Y. Ohno, M. Maekawa and M. Munakata, *Inorg. Chem.*, 1997, **36**, 6382.
5 K. Biradha, Y. Hongo and M. Fujita, *Angew. Chem., Int. Ed. Engl.*, 2000, **39**, 3843.
6 M. J. Zaworotko, *Angew. Chem., Int. Ed.*, 2000, **39**, 3052.
7 M. Fujita, Y. J. Kwon, S. Washizu and K. Ogura, *J. Am. Chem. Soc.*, 1994, **116**, 1151.
8 M. Fujita, K. Umemoto, M. Yoshizawa, N. Fujita, T. Kusukawa and K. Birdha, *Chem. Commun.*, 2001, 509.
9 M. Eddaoudi, D. B. Moler, H. Li, B. Chen, T. M. Reineke, M. O'Keeffe and O. M. Yaghi, *Acc. Chem. Res.*, 2001, **34**, 319.
10 L. R. MacGillivary, S. Subramanian and M. J. Zaworotko, *J. Chem. Soc., Chem. Commun*, 1994, 1325.
11 F. Robinson and M. J. Zaworotko, *J. Chem. Soc., Chem. Commun.*, 1995, 2413.
12 M. Fujita, Y. J. Kwon, O. Sasaki, K. Yamaguchi and K. Ogura, *J. Am. Chem. Soc.*, 1995, **117**, 7287.
13 P. Losier and M. J. Zaworotko, *Angew. Chem., Int. Ed. Engl.*, 1996, **35**, 2779.
14 O. M. Yaghi, H. Li, C. Davis, D. Richardson and T. L. Groy, *Acc. Chem. Res.*, 1998, **31**, 474.
15 C. J. Kepert and M. J. Rosseinsky, *Chem. Commun.*, 1999, 375.
16 K. Birdha, A. Mondal, B. Moulton and M. J. Zaworotko, *J. Chem. Soc., Dalton Trans.*, 2000, 3837.
17 COLLECT, data collection software, Nonius, Delft, 1998.
18 Z. Otwinowski and W. Minor, Processing of X-ray Diffraction Data Collected in Oscillation Mode, *Methods in Enzymology*, vol. 276: Macromolecular Crystallography, part A, ed. C. W. Carter, Jr. and R. M. Sweet, Academic Press, 1997, p. 307.
19 G. M. Sheldrick, SHELX-86, in Crystallographic Computing 3, ed. G. M. Sheldrick, C. Kruger and R. Goddard, Oxford University Press, Oxford, 1985, p. 175.
20 G. M. Sheldrick and T. R. Schneider, SHELXL: High-Resolution Refinement, *Methods in Enzymology*, **vol. 277** Macromolecular Crystallography Part B, ed. C. W. Carter and R. M. Sweet, 1997, p. 319.
21 L. J. Barbour, X-SEED, A Graphical Interface to SHELX, University of Missouri, Columbia, USA, 1999.
22 K. Yvon, W. Jeitschko and E. Parthe, *J. Appl. Crystallogr.*, 1977, **10**, 73.
23 L. J. Barbour, SECTION, A Computer Program for the Graphic Display of Cross Sections Through a Unit Cell, *J. Appl. Crystallogr.*, 1999, **32**, 353.
24 K. Nakamoto, in *Infrared and Raman Spectra of Inorganic and Coordination Compounds*, Wiley, New York, 1978, ch. 3, p. 270.
25 B. Żurowska, J. Mroziński, M. Julve, F. Lloret, A. Maslojeva and W. Sawska-Dobrowolska, *Inorg. Chem.*, 2002, **41**, 1771.
26 M. R. Caira, L. R. Nassimbeni, F. Toda and D. Vujovic, *J. Am. Chem. Soc.*, 2000, **122**, 936.
27 M. R. Caira, L. R. Nassimbeni, in *Comprehensive Supramolecular Chemistry*, ed. J. L. Atwood, J. E. D. Davies, D. D. MacNicol and F. Vögtle, Elsevier Science, Oxford, vol. 6, ch. 25, p. 825.
28 J. L. Atwood, L. J. Barbour and A. Jerga, *Science*, 2002, **296**, 2367.
29 R. D. Archer, in *Inorganic and Organometallic Polymers, Special Topics in Inorganic Chemistry*, ed. R. B. King, Wiley-VCH, New York, 2001, ch. 1, p. 20.
30 H. Nierengarten, J. Rojo, E. Leize, J.-M. Lehn and A. Van Dorsselaer, *Eur. J. Inorg. Chem.*, 2002, 573.
31 R. D. Archer, in *Inorganic and Organometallic Polymers, Special Topics in Inorganic Chemistry*, ed. R. B. King, Wiley-VCH, New York, 2001, ch. 3, p. 93.
32 I. Haiduc and F. T. Edelmann, in *Supramolecular Organometallic Chemistry*, Wiley-VCH, Weinheim, 1999.